International Journal for Housing Science and Its Applications
Publish August 10, 2025. Volume 46, Issue 4 Pages 2014-2027

https://doi.org/10.70517/ijhsa464173

Consideration of a multi-objective reactive power compensation optimization model for active distribution grids with distributed energy access

Jingjing Gao[1,*]
[1] College of Electrical and Information Engineering, Heilongjiang Institute of Technology, Harbin, Heilongjiang, 150000, China
Corresponding authors: (e-mail: gao_jingjing1996@163.com).

Abstract Under the large-scale access of distributed energy resources to the distribution network, the stochasticity and volatility of energy generation have gradually become the main difficulties in the optimized and stable operation of system voltage and reactive power. Based on the structure and characteristics of active distribution network, this paper takes network loss, voltage deviation and economic index of equipment regulation as the objective function of distribution network optimization, and selects current, node voltage and energy storage as the constraints to form a multi-objective reactive power optimization model of active distribution network. At the same time, Circle chaotic initialization, sinusoidal cosine algorithm and Cauchy variational perturbation are used to improve the standard sparrow search (SSA) algorithm, and the improved sparrow search (ISSA) algorithm based on multi-strategy fusion is proposed. By applying the model and solution method proposed in this paper to the scenery scenario, it can assist in decreasing the network loss expense by up to 36.53% and voltage offset by up to 24.34%.

Index Terms multi-objective reactive power optimization, improved sparrow search algorithm, distributed energy, active distribution network

I. Introduction

With the increasing depletion of fossil energy sources such as oil and coal as well as the intensification of the global climate and environmental crisis, the vigorous development of renewable and clean energy has become an important strategic program for sustainable economic and social development [1], [2]. As a typical representative of distributed power generation, solar energy, wind energy and other new energy field stations have the advantages of high degree of automatic control, flexible configuration, environmental protection and non-pollution, which are favored and vigorously promoted by various countries [3]-[5]. According to statistics, in developed countries, the annual new installed capacity of the total capacity of new energy generating units accounted for more than 60% [6]. Since the new century, a new round of energy revolution has been set off around the efficient development and utilization of clean energy such as wind and light [7]. In the context of global environment as well as energy issues, distributed generation (DG) based on renewable energy has become an important way to transform the structure of energy consumption and realize sustainable development [8]-[11]. DG usually refers to power generation units that are installed near the users and have an installed capacity of power supply ranging from a few kilowatts to tens of megawatts [12], [13]. Currently, the development of DG technology represented by photovoltaic (PV) and wind power (WP) is relatively mature, which has the advantages of flexible installation location, and is green, efficient, and economical [14].

So far, DG has been more widely used in power distribution systems, which plays an important role in reducing carbon emissions and fossil energy consumption [15]. However, the uncertainty of DG output also brings a lot of challenges for distribution network dispatch operation. Take photovoltaic as an example, the light intensity fluctuates frequently, and the correlation between PV output and light intensity is strong, and the uncertainty of PV output is large, which has a large impact on the distribution network current, node voltage, peak regulation, frequency regulation, etc [16]-[19]. If the traditional passive mode of fit-and-forget is adopted in distribution network operation, ignoring the uncertainty of PV output, it will lead to the increase of the actual investment and operation cost of the distribution network, the rate of light abandonment and network loss, and it is difficult to give full play to the role of new energy in the distribution network [20].

To solve the above problems, active distribution network (AND) technology has emerged [21], [22]. ADN provides active control of broad distributed energy resources (DERs) such as DGs, energy storage systems, flexible loads, reactive power compensation devices, etc., and realizes flexible and active operation of distribution networks [23]-[25]. In practice, the goals of AND operation and scheduling are usually diverse, including reducing network losses, reducing voltage deviation, improving renewable energy utilization, and reducing operating costs, etc., and these goals are often intertwined or even contradictory in time and space, so it is difficult to apply and promote them in actual projects if an inappropriate operation method is selected [26]. In summary, the study of active distribution network multi-objective reactive power compensation optimization taking into account the uncertainty of DG output can not only meet the requirements of multiple operational objectives in ADN, but also make the scheduling and operation mode able to flexibly cope with the impact of uncertainty of DG output, which is of great significance to the actual operation of distribution networks.

There are more types of control variables in AND, such as new energy inverter, on-load voltage regulator transformer and capacitor bank, etc., and the reactive power compensation optimization results are affected by each control variable, so it is necessary to comprehensively consider the state of each control variable [27]. In addition, the wide range of values of control variables in reactive power optimization and the complexity of system operation constraints lead to the fact that reactive power optimization for active distribution networks is a nonlinear optimization problem with many objective functions and constraints, and complex types of variables [28]. So far, traditional reactive power optimization algorithms and artificial intelligence optimization algorithms are the two commonly used solutions for reactive power optimization problems.

(1) Traditional reactive power optimization algorithm

The traditional reactive power optimization algorithms are developed relatively early, and they only solve problems with low complexity, and the optimization strategies are relatively simple, mainly including linear programming method, nonlinear programming method and dynamic programming method.

For the linear programming method, it first performs a Taylor expansion of the objective function and constraints, and then omits the higher terms, thus transforming the original problem into a linear programming problem [29]. Xu, P et al [30] proposed a linear programming method for optimizing the parameters of dynamic reactive power compensation devices to improve the security in distributed new energy power systems and to increase the inter-area power transmission capacity. Zhang, C et al [31] explored the optimization of reactive power compensation under interval uncertainty by proposing a linear approximation method combined with an improved version of affine arithmetic and compared its effectiveness with other methods. Qu, L et al [32] proposed a multi-objective reactive power optimization method for renewable power generation based on a mixed integer optimization technique with semidefinite programming. The method uses time and space grouping model to achieve stabilization of bus voltage and reduce network losses. These methods require high data accuracy and are computationally intensive.

The nonlinear planning method uses the tidal equations as constraints and transforms the original problem into solving a system of nonlinear equations by introducing slack variables and augmenting the objective function [33]. Amrane, Y et al [34] developed a new tool for optimizing reactive power resources in power systems based on particle swarm optimization algorithm in conjunction with the nonlinear interior-point method and tested the tool on an IEEE57 node system to demonstrate the effectiveness of the tool. Soler, E et al [35] proposed a penalty-based nonlinear solver for efficiently handling discrete variables in the optimal reactive power scheduling problem to be continuous and differentiable, and verified its effectiveness through simulation experiments. The mathematical model of this type of method is more intuitive and the computational accuracy is high, but the computational scale is large and the stability is not good.

The dynamic programming method leads to the optimal solution of the master problem step by step from the optimal solution of the subproblems [36]. Rather, Z et al [37] proposed a mixed-integer dynamic optimization method for optimal dynamic reactive power allocation to improve the voltage security and system capacity for the dynamic security problem that exists when large-scale wind energy sources are connected to the distribution network. Paramasivam, M et al [38] proposed a dynamic optimization method based on parameterization of control vectors to ensure short-term voltage stability of the power system through optimal deployment of dynamic reactive resources and to solve problems caused by induction motor loads. Shen, X et al [39] proposed a new dynamic reactive power optimization method which simplifies the complex programming problem by utilizing heuristic searches and variable corrections, and demonstrated its superiority over conventional methods by evaluating it on the IEEE grid system. Such methods can improve the solution efficiency by using practical knowledge and experience, but problems such as modeling complexity and dimensionality catastrophe occur with the increase in the number of variables.

All of the above algorithms have a solid mathematical foundation, are theoretically mature, and have a fast computational speed, but there is a certain lack of ability to search for the global optimal solution. In addition, due to the fact that there are more discrete variables in the reactive power compensation optimization process of AND,

and the general methods require that they can be microscopic or linearizable, so the continuous solutions obtained by these methods will still have some errors in the discrete variables obtained after processing. To address these problems, researchers have gradually turned their attention to artificial intelligence algorithms.

(2) Artificial Intelligence Based Multi-Objective Reactive Power Compensation Optimization Model for AND

In order to find algorithms that can quickly and accurately solve complex reactive power optimization models, researchers have proposed a series of heuristic artificial intelligence search algorithms based on the inspiration of nature [40]. These algorithms have the advantages of fast search speed, simple optimization conditions as well as easy programming implementation, and they can directly solve nonlinear optimization problems with mixed integers [41]. Sarvaiya, J et al [42] proposed a multi-objective optimization strategy based on heuristic algorithms (Particle Swarm Optimization Algorithm, Optimization Algorithm based on Linear Approximation, and Genetic Algorithm) for a 56-node distribution network to to implement reactive power compensation to minimize active power losses and improve voltage distribution for better economic efficiency. Linlin, Y et al [43] proposed a multi-objective reactive power optimization model based on the Gray Wolf algorithm aiming to improve the voltage quality and system stability of AND with a high share of new energy sources such as wind power and PV. Dong, P et al [44] proposed a multi objective reactive power coordinated control model aimed at solving the problems of insufficient coordination and high active power losses in reactive power compensation devices, which employs an improved NSGA-II algorithm to find the optimal control strategy. Ganguly, S [45] proposed a multi-objective planning algorithm based on partial swarm intelligent optimization for reactive power compensation optimization in radial distribution networks, which employs unified power quality regulator assignment to optimize UPOC ratings, network power losses, and undervoltage problems.

In this paper, we first describe the structural components of the active distribution network system, build the distribution network branch current model and derive the constraints. On this basis, the mathematical operations of multi-objective reactive power optimization objective function and constraints are described in detail, and the multi-objective reactive power optimization model is established. Secondly, the improved sparrow search algorithm based on strategy fusion is designed to demonstrate the solution process of ISSA algorithm applied to the multi-objective reactive power optimization model. Again, 10 simulation scenarios are set up to explore the impact of distributed PV grid connection on the voltage distribution and network loss of the distribution network based on the model and method proposed in this paper. Finally, the scenarios are generated and the reactive power compensation points are screened to compare the compensation effect before and after the application of the model and method in this paper.

II. Establishment of multi-objective reactive power optimization model

II. A.Active distribution network structure

The active distribution network contains distributed power sources, energy storage, loads and related control systems. Active distribution network has active scheduling function, so it can actively mobilize the control structure to carry out effective self-regulation, so as to realize the active distribution network safe, stable and economic operation. The traditional distribution network contains various voltage regulating devices, so the voltage regulating devices should also work together with the active distribution network to realize the voltage coordination and optimization of the active distribution network.

Active distribution grid has high effect on energy storage and distributed power consumption:

(1) Under the active management and active control characteristics of active distribution network and the conditions that energy storage balances distributed power supply and distributed power supply output, the phenomenon of wind and light abandonment is greatly mitigated, which improves the consumption capacity of distributed power supply.

(2) active distribution network and user side contact is closer, it can be load side scheduling, in the situation of time-sharing tariffs can give full play to the load side to participate in the grid regulation capabilities, such as peak shaving to fill in the valley, to improve the active distribution network security and reliability.

The active distribution network trend modeling, the optimal trend is generally optimized through its adjustable equipment, and adjustable equipment control and coordination requires a very complex operating strategy, therefore, how to model the ADN and can be solved efficiently and quickly is the focus of the study, the proposed radial grid branch trend model, then, a single radial line structure is shown in Figure 1.

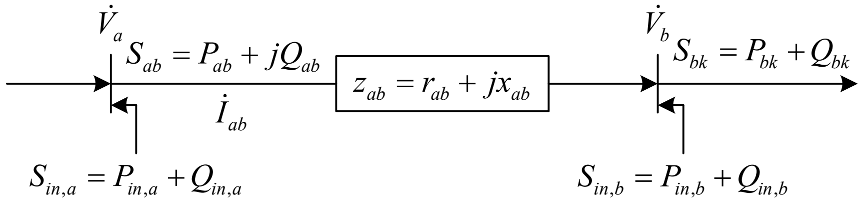

Figure 1: Branch power flow model of distribution network

In Fig. 1, $\dot{V}_a$: Voltage at node a. $\dot{V}_b$: Voltage at node b. $\dot{I}_{ab}$: Current of the line. $r_{ab} + jx_{ab}$: Impedance of the line. $P_{ab} + jQ_{ab}$: Apparent power on the side of node a. $P_{in,a}$: Injected active power at node a. $Q_{in,a}$: Injected reactive power at node a. The following active distribution network current model constraints are derived from a simple radial line structure diagram with constraints as in Eqs. (1)-(3).

$$\dot{V}_b - \dot{V}_a = z_{ab}\dot{I}_{ab} \tag{1}$$

$$S_{ab} = \dot{V}_a \cdot \dot{I}_{ab}^* \tag{2}$$

$$S_b = \sum_{k:b\to k} S_{bk} - \sum_{a:a\to b}\left(S_{ab} - z_{ab}\left|\dot{I}_{ab}\right|^2\right) \tag{3}$$

Since Eqs. (2) and (3) are in nonlinear form, where $\dot{I}_{ab}^*$ denotes the conjugate of current $\dot{I}_{ab}$. Therefore first it is necessary to relax it into nonlinear form and here phase angle relaxation is used to relax it. Since the current problem is a minimization problem, and for the minimization problem, the optimal value f' of the optimization problem after relaxation is the lower bound of the optimal value f of the original problem, i.e., $f' \le f$, if $f = f'$, then the relaxation is tight. Then the phase angle relaxation is also tight for it, and the transformation process is as follows: first remove the phase angle of the voltage and current, so that $l_{ab} = \left|\dot{I}_{ab}\right|^2$. $v = \left|\dot{V}\right|^2$. where, v_a: the square of the voltage magnitude at node a. l_{ab}: Square of the line current magnitude. $k: b \to k$: Sub-node of node b.

Substituting $S_{ab} = V_a \cdot \dot{I}_{ab}^*$ into Eq. (1) yields Eq. (4).

$$\dot{V}_b = \dot{V}_a - z_{ab} \cdot \frac{S_{ab}^*}{\dot{V}_a^*} \tag{4}$$

Eq. (4) is multiplied by its own conjugate at each end to obtain Eq. (5).

$$\begin{aligned} v_b = \dot{V}_b \cdot \dot{V}_b^* &= \left(\dot{V}_a - z_{ab} \cdot \frac{S_{ab}^*}{V_a^*}\right) \cdot \left(\dot{V}_a^* - z_{ab}^* \cdot \frac{S_{ab}}{V_a}\right) \\ &= v_a - 2\left(r_{ab}P_{ab} + x_{ab}Q_{ab}\right) - \left(r_{ab}^2 + x_{ab}^2\right)l_{ab} \end{aligned} \tag{5}$$

Eq. (1) is transformed into Eq. (6).

$$v_a - v_b = 2\left(r_{ab}P_{ab} + x_{ab}Q_{ab}\right) - \left(r_{ab}^2 + x_{ab}^2\right)l_{ab} \tag{6}$$

Eq. (3) is split into active and reactive components as in Eqs. (7)-(8).

$$P_{in,a} = \sum_{k:b\to k} P_{bk} - \left(P_{ab} - l_{ab}r_{ab}\right) \tag{7}$$

$$Q_{in,a} = \sum_{k:b\to k} Q_{bk} - \left(Q_{ab} - l_{ab}x_{ab}\right) \tag{8}$$

and Eq. (2) transforms to Eq. (9):

$$l_{ab}v_a = P_{ab}^2 + Q_{ab}^2 \quad l_{ab} \ge 0 \tag{9}$$

Since Eq. contains squared terms, it is still not a convex optimization problem and needs to be relaxed even further, i.e., it is optimized using second-order cone relaxation techniques.

The safe operation constraints of the active distribution network are shown below.

The node voltage squared operation constraint is shown in Eq. (10).

$$v_{a,\min} \le v_a \le v_{a,\max} \ \forall a \in N \tag{10}$$

The branch current squared operation constraint is shown in equation (11).

$$l_{ab} \le l_{ab,\max} \ \forall a \in N \tag{11}$$

The node active power constraint is shown in equation (12).

$$P_{a,\min} \le P_a \le P_{a,\max} \ \forall a \in N \tag{12}$$

The node reactive power constraint is shown in equation (13).

$$Q_{a,\min} \le Q_a \le Q_{a,\max} \ \forall a \in N \tag{13}$$

The active power balance constraint for each time period is shown in equation (14).

$$P_a + P_{load} - P_g - P_{wt} - P_{dch} + P_{ch} - P_{pvu} + P_{TSL} - P_{IL} = 0 \ \forall a \in N \tag{14}$$

where, P_{load}: Active load. P_g: Generator active power. P_{wt}: Wind turbine active power. P_{dch}: Energy storage discharge power. P_{ch}: Energy storage charging power. P_{pvu}: Photovoltaic power. P_{TSL}: Time-shiftable load power. P_{IL}: Interruptible load power.

The reactive power balance constraints for each time period are shown in equation (15).

$$Q_a + Q_{load} - Q_g - Q_{CB} - Q_{SVC} == 0 \ \forall a \in N \tag{15}$$

where, Q_{load}: reactive power load, Q_g: generator reactive power, Q_{CB}: CB reactive power, Q_{SVC}: SVC reactive power.

II. B. Multi-objective reactive power optimization objective function and constraints

II. B. 1) Objective function

(1) Network loss

Minimum active network loss is currently the most used objective function in reactive power optimization, which can be expressed as equation (16):

$$\min F_1 = \min \sum_{t=0}^{23} \left[\sum_{i=1, j\in k}^{n} G_{ij} \times \left(U_i^2 + U_j^2 - 2U_i U_j \cos\theta_{ij} \right) \right] \tag{16}$$

where, U_i is the voltage at node i. U_j is the voltage of node j. k is the set of nodes directly connected to node i. G_{ij} is the conductance. θ_{ij} is the voltage phase difference.

(2) Voltage deviation

Because a large number of distributed energy sources are connected to the distribution network, so that the law of energy flow in the network will be changed, which causes the voltage deviation in the distribution network. So in order to keep the voltage offset range from being too large, the minimum voltage deviation is taken as the objective function. That is, equation (17):

$$\min F_2 = \min \sum_{t=0}^{23} \left[\sum_{i=1}^{n} \left(U_i - U_i^{\exp} \right)^2 \right] \tag{17}$$

where, $U_i^{\exp}$ is the desired value of node i voltage.

(3) Economy of device regulation

As it relates to the economics of distribution network operation, the economics of each reactive power compensation device must also be considered. The following is the economy function of reactive power compensation devices, i.e., Eq. (18):

$$f_n = \sum_{i=1}^{N_T} S_{T_i} \Delta u_{T_i} + \sum_{j=1}^{N_C} S_{C_j} \Delta u_{C_j}, i \in N_T, j \in N_C \tag{18}$$

where, N_T is the set of distributed power sources. N_C is the set of reactive power compensation devices. S_{T_i} is the regulation cost per unit change of the i th distributed power supply. Δu_{T_i} is the regulation change of the unit change of the distributed power supply of the first unit. S_{C_j} is the regulation cost per unit change of the j th reactive power compensation device. Δu_{C_j} is the regulation change per unit of change of the first reactive power compensation device.

II. B. 2) Constraints

(1) Currents are constrained as in equation (19):

$$\begin{cases} \Delta P_i - U_i \sum_{j=1}^{n} U_j \left(G_{ij} \cos\theta_{ij} + B_{ij} \sin\theta_{ij} \right) = 0 \\ \Delta Q_i - U_i \sum_{j=1}^{n} U_j \left(G_{ij} \sin\theta_{ij} - B_{ij} \cos\theta_{ij} \right) = 0 \end{cases} \tag{19}$$

where ΔP_i and ΔQ_i are the combined active and reactive values of the loads at node i, the distributed power sources and the compensation equipment, respectively. B_{ij} is the electricana of the line between nodes i and j.

(2) The node voltage constraint is shown in equation (20):

$$U_{i,\min} \le U_i \le U_{i,\max} \tag{20}$$

where, $U_{i,\min}$ is the minimum system voltage. $U_{i,\max}$ is the maximum system voltage.

(3) Distributed power constraints

At the time of DG access, certain constraints are also imposed on the output of the DG for better reactive power optimization. The output power constraint is shown in equation (21):

$$\begin{cases} P_{iDG,\min} \le P_{iDG} \le P_{iDG,\max} \\ Q_{iDG,\min} \le Q_{iDG} \le Q_{iDG,\max} \end{cases} \tag{21}$$

where, $P_{iDG,\min}$ is the minimum active power output from the distributed power supply. $P_{iDG,\max}$ is the maximum active power output from the distributed power supply. $Q_{iDG,\min}$ is the minimum reactive power output from the distributed power supply. $Q_{iDG,\max}$ is the maximum reactive power output from the distributed power supply.

(4) Power factor constraint of reactive power compensation device

If the power factor of the reactive power compensation device in the system is too low due to the output of reactive power, this does not comply with the power factor regulations in the distribution network. So the power factor constraints are to be set on the reactive power compensation device as in equations (22)-(23):

$$Q_{\min} \le Q \le Q_{\max} \tag{22}$$

$$\cos\varphi_{\min} \le \cos\varphi \tag{23}$$

where $Q_{\min}$ is the minimum compensation amount of the reactive power compensation device. $Q_{\max}$ is the maximum compensation amount of the reactive power compensation device. $\cos\varphi_{\min}$ is the minimum power factor of the reactive power compensation device, which cannot be lower than 0.9 according to national regulations.

III. Active distribution network optimization based on improved sparrow search algorithm

III. A. Principle of Improved Sparrow Search Algorithm Based on Multi-Strategy Fusion

Compared with most intelligent optimization algorithms, SSA has certain advantages in solving optimization models. However, with the increase of the complexity of the solving model, there still exists the problem of low convergence accuracy and difficulty in jumping out of the local optimal solution. Especially for the distribution network reactive power optimization mathematical model containing distributed power sources, the grid connection of distributed power sources increases the difficulty of solving the reactive power optimization mathematical model. To solve this problem, ISSA based on multi-strategy fusion is proposed, aiming to improve the algorithmic performance of SSA to cope with the reactive power optimization mathematical model of more complex scenarios.

(1) Circle chaotic mapping initialization

SSA adopts the random number generation method in the process of initializing the population, which is prone to make the initial population unevenly distributed, affecting the speed and accuracy of the later iteration. The initialized population based on chaotic mapping has the characteristics of traversability and randomness. Circle chaotic mapping is used to initialize the sparrow population with the expression of equation (24):

$$x_{i+1} = \operatorname{mod}\left(x_i + 0.2 - \left(\frac{0.5}{2\pi}\right)\sin(2\pi \cdot x_i), 1\right) \tag{24}$$

where mod is the residual function.

In the comparison of Circle chaotic mapping and random distribution, when the iterative calculation of Circle chaotic mapping and random distribution is 200 times respectively, the initialized population generated by Circle chaotic mapping is more uniformly distributed compared with random distribution, so that the sparrow population has a wider search space, which improves the accuracy of the algorithm at the beginning of the iteration.

(2) Fusion of sine-cosine algorithm idea

Compared with PSO, GWO, etc., SSA has a more superior convergence speed, but it is easy to fall into local optimum when solving high-dimensional optimization models. From the standard SSA to get the finder position update formula, it can be seen that when $R_2 < ST$, the sparrow position will eventually converge to 0, which greatly limits the search space of the sparrow population in the late iteration. For this reason, the sine-cosine algorithm position is introduced to update the finder's position.

The amplitude conversion factor r_1 of the traditional sine-cosine algorithm shows a linear decreasing trend, which is not suitable for algorithm optimization. The improved amplitude conversion factor is shown in equation (25):

$$r_{1'} = \sqrt[\eta]{1-\left(t / Iter_{\max}\right)^{\eta}} \tag{25}$$

where t is the current iteration number, η is the adjustment factor, and $\eta \geq 1$.

The improved amplitude conversion factor r_1' is larger and decreasing slowly in the pre iteration period, which is easy to search globally, and smaller and decreasing fast in the late iteration period, which is easy to search locally over short distances. Then the new finder position is obtained updated as in equation (26):

$$X_{i,d}^{t+1} = \begin{cases} X_{i,d}^{t} + r_1' \cdot \sin(r_2) \cdot \left| r_3 X_{best}^{t} - X_{i,j}^{t} \right| & R_2 < ST \\ X_{i,d}^{t} + r_1' \cdot \cos(r_2) \cdot \left| r_3 X_{best}^{t} - X_{i,j}^{t} \right| & R_2 \geq ST \end{cases} \tag{26}$$

where $X_{i,d}^{t}$ denotes the position of the i rd sparrow in the j th dimension at the t nd iteration. X_{best} denotes the global best position of the current sparrow population, r_2 and r_3 denote random numbers within the interval of $[0, 2\pi]$, R_2 and ST denote the warning and safety values, $R_2 \in [0,1]$, $ST \in [0.5,1]$, respectively.

(3) Cauchy Variation Perturbation

Perturbation mechanisms are usually used to overcome the problem that AI algorithms are prone to fall into local optimality in the late iteration, among which Cauchy's variation and Gaussian variation are two common perturbation mechanisms. The Cauchy density function approaches 0 at a slower rate, which is not only beneficial for the sparrow population to jump out of the local optimum, but also increases the variability between parents and offspring. Therefore, the perturbation method using the Cauchy variation is beneficial for the intelligent optimization algorithm to jump out of the local optimum at the later stage of the iteration.

In high-dimensional complex optimization models, SSA is prone to sparrow populations gathering in the local optimum and difficult to jump out at the late iteration, which reduces the diversity of populations at the late iteration of the algorithm. To cope with such problems, this paper proposes to introduce the Cauchy variation perturbation mechanism, which performs the Cauchy variation operation on the optimal solution obtained in each iteration to improve the global search capability of the sparrow population. The formulas for perturbing the global optimal solution using Cauchy variation are shown in Eqs. (27)-(28):

$$X_{i,d}^{t+1} = X_{best}^{t} + Cauchy(0,1) \otimes X_{best}^{t} \tag{27}$$

$$Cauchy(0,1) = \tan\left(\left(rand - 0.5\right) \cdot \pi\right) \tag{28}$$

where $rand$ denotes a random number between $[0,1]$. $Cauchy$ denotes the value of the random perturbation of the standard Cauchy variant.

III. B. Solution flow of reactive power optimization model for active distribution network

As can be seen from the previous subsection, the implementation of ISSA in this paper is mainly divided into three phases: the first phase initializes the sparrow population and calculates the fitness function through Circle chaotic mapping. In the second stage, the position update is performed through the respective position update formulas of the three types of sparrow populations, in which the finder position update incorporates the idea of sine-cosine algorithm. In the third stage, the current global optimum is perturbed using the Cauchy variation to improve the population diversity at the later stage of the iteration to obtain the final solution.

The application of ISSA to the distribution network reactive power optimization process is shown in Fig. 2, and the specific steps are as follows:

Step 1: In the day-ahead stage, obtain the basic parameters of the distribution network as well as the future 24-hour active forecast data of photovoltaic, wind power and loads to establish the optimization model.

Step 2: Set the basic parameters of the algorithm such as sparrow population size n, maximum number of iterations $T_{\max}$, the ratio of discoverers, joiners and scouts, warning value R_2, and security value ST.

Step 3: Initialize the sparrow population using Circle chaotic mapping, calculate the fitness value and sort it.

Step 4: Update the finder position and update the joiner and scout.

Step 5: Calculate the fitness value and update the sparrow position.

Step 6: Perturb the optimal sparrow with Cauchy variation.

Step 7: Determine whether the current number of iterations reaches the maximum number of iterations, if it reaches the maximum number of iterations, output the optimal solution of the day-ahead reactive optimization as well as the decision values of each decision variable, otherwise return to Step 4.

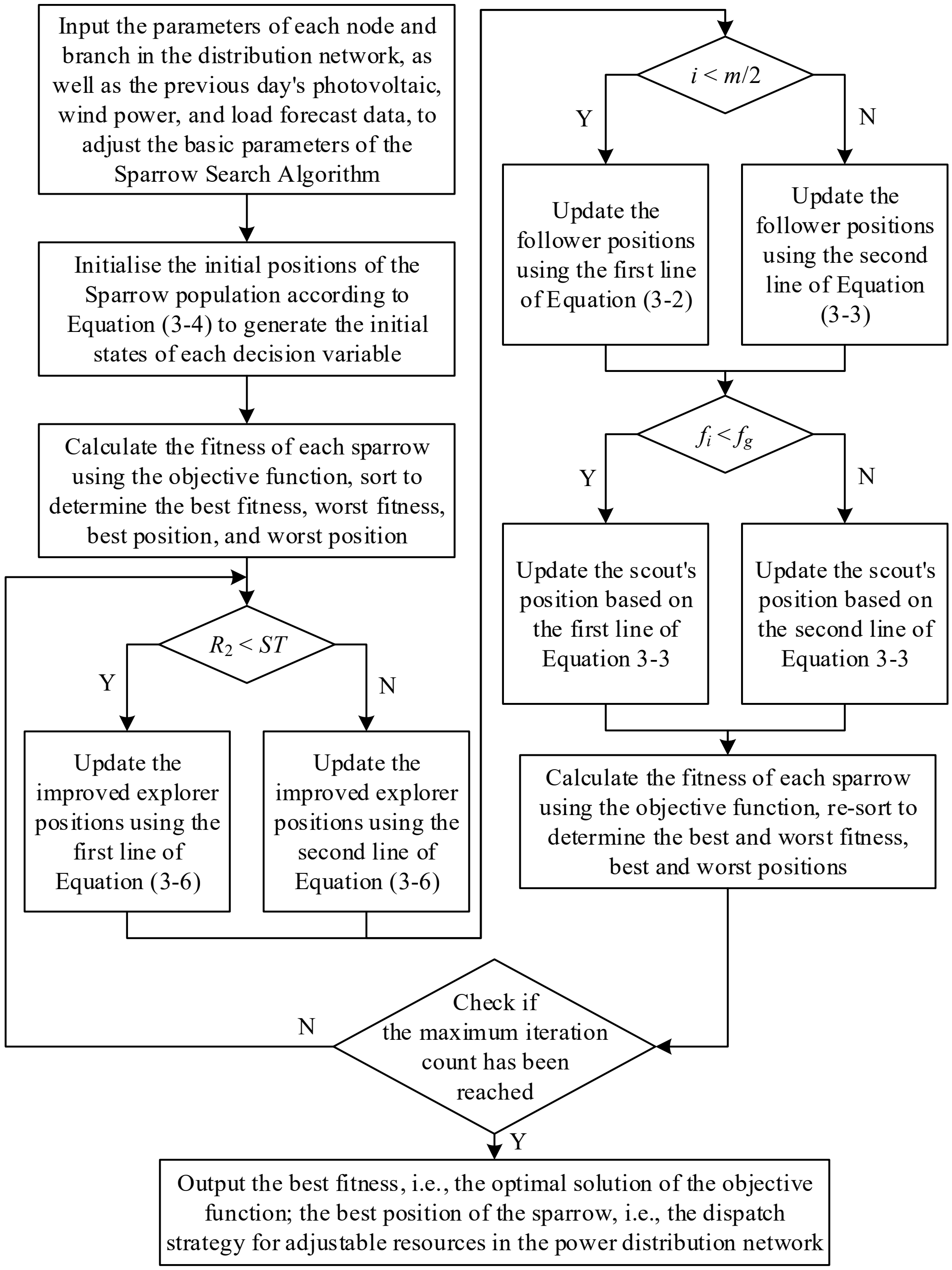

Figure 2: The reactive power optimization process of ISSA's distribution network

IV. Simulation and application of multi-objective reactive power optimization model and solution

In this chapter, a standard IEEE 33-node standard distribution network system is used as an experimental object for simulation experiments and practical applications supported by the objective-free reactive power optimization model and solution method designed in this paper. The distribution network has 33 nodes and 32 branch circuits, and the initial voltage of each node is 1.0 p.u., and the allowable voltage fluctuation range is ±7% of the nominal voltage. Ten simulation schemes are set up as follows:

(A1) Scenario 1: Decentralized access with 30% PV penetration and 280.0kW per node network capacity.
(A2) Scenario 2: First end of feeder access with 30% PV penetration and 280.0kW per node network capacity.
(A3) Scenario 3: Feeder end access with 30% PV penetration and 280.0kW per node network capacity.
(A4) Scenario 4: Branch node access with 30% PV penetration and 380.0kW per node network capacity.
(A5) Scenario 5: Decentralized access with 70% PV penetration and 660.0kW per node network capacity.
(A6) Scenario 6: Decentralized access with 100% PV penetration and a network capacity of 930.0kW per node.

(A7) Scenario 7: Decentralized access with 200% PV penetration and a network capacity of 1860.0kW per node.

(A8) Scenario 8: End-of-feeder access with 70% PV penetration and a network capacity of 660.0kW per node.

(A9) Scenario 9: End-of-feeder access with 100% PV penetration and a network capacity of 930.0kW per node.

(A10) Scenario 10: End-of-feeder access with 200% PV penetration and a network capacity of 1860.0kW per node.

IV. A. Example analysis

IV. A. 1) Voltage distribution

When the PV penetration rate of 30%, decentralized access, the first end of the feeder access, branch node access and decentralized access to a total of four different access modes when the distribution network voltage distribution is shown in Figure 3, where "A0" for the non-access to the DG state.

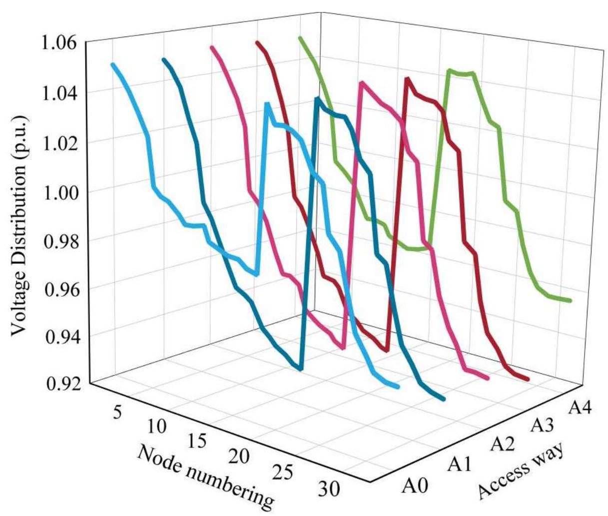

Figure 3: The voltage distribution when the photovoltaic penetration rate is 30%

The voltage distribution of the distribution network when PV is connected at decentralized access and at the end of the feeder is shown in Fig. 4.

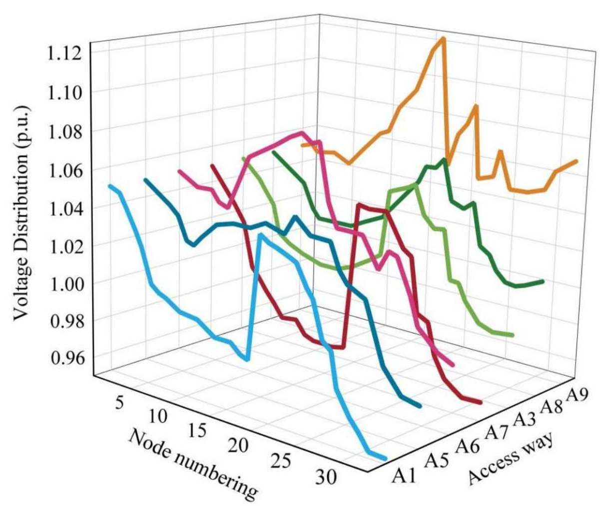

Figure 4: Voltage distribution of the distribution network

By observing and analyzing Figures 3 and 4 the following conclusions can be drawn:

(1) The order of voltage support to the distribution network by the four access methods: decentralized access > feeder end access > branch node access > feeder first end access.

(2) If decentralized access is used, DG has a stronger role in supporting the voltage of feeder 1 and a weaker role in supporting the voltage of feeders 2 and 3. If the feeder end access method is used, the reverse is true.

Decentralized access and end-of-feeder access two access methods for feeder 4 voltage support role is basically flat.

(3) When the PV penetration rate is small, decentralized access or end-of-feeder access should be used to improve the overall voltage level of the distribution network, which should be further selected in combination with the PV penetration rate and the voltage quality requirements for each feeder. When the PV penetration rate is too large, branch node access or even feeder end access should be used to minimize the number of nodes of the distribution network with the upper voltage limit.

IV. A. 2) Changes in network losses

The above algorithm is to study the effect of one variable, PV penetration rate, on the network losses of the distribution network under the condition that the grid-connection location variable is fixed. In order to combine the PV penetration rate and grid-connected location to analyze the change of network loss of distribution network under the condition of individual distributed PV access, this example takes the PV penetration rate and grid-connected location as variables, and a total of 130 scenarios are tested, and the simulation and analysis results of individual scenarios are plotted as a surface of network loss in Fig. 5.

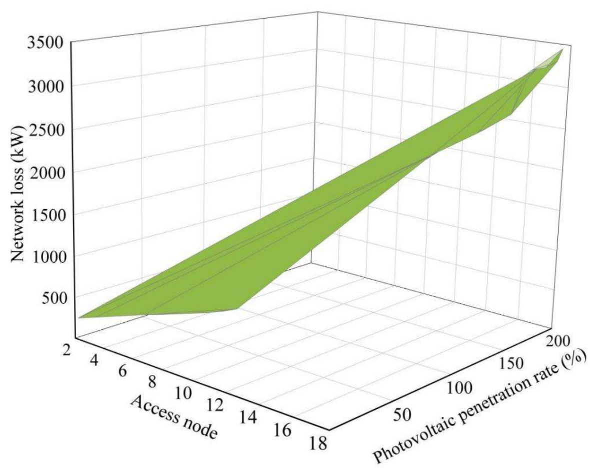

Figure 5: Network loss at different penetration rates and grid connection locations

The surface plot of network losses with respect to PV penetration rate and grid connection location is banded concave, which can also be concluded from Fig. 5:

(1) For any grid-connected location in any distribution network, there exists an optimal grid-connected penetration rate that produces the minimum value of network losses.

(2) As the PV grid-connected location continues to approach the end of the feeder, the PV penetration rate that minimizes network losses in the distribution network decreases.

(3) As the PV penetration rate continues to increase, the grid-connected location that minimizes the network loss of the distribution network will gradually move closer to the first end of the feeder. Through this surface diagram, we can have a more in-depth understanding of the pattern of change of network loss after the distributed PV power supply is connected to the distribution network.

IV. B. Practical Scenario Applications

IV. B. 1) Landscape Scene Generation

Taking one year of 8880h wind data from the Q regional power grid as an example, K typical scenes are generated by means of loop iteration with the objective of minimizing the distance from the sample profile coefficients to the maximum profile value. When the integrated sample points whose contour coefficients are closest to the optimal value, the clustering effect is better globally. In order to avoid the influence of local convergence and the sensitivity of the initial center of mass selection on the clustering effect, and at the same time to make the global clustering effect optimal, i.e., S is minimized, K=74 is selected as the number of typical scenes see Fig. 6(a), and the production of the typical scenes is calibrated for the profile coefficients in Fig. 6(b).

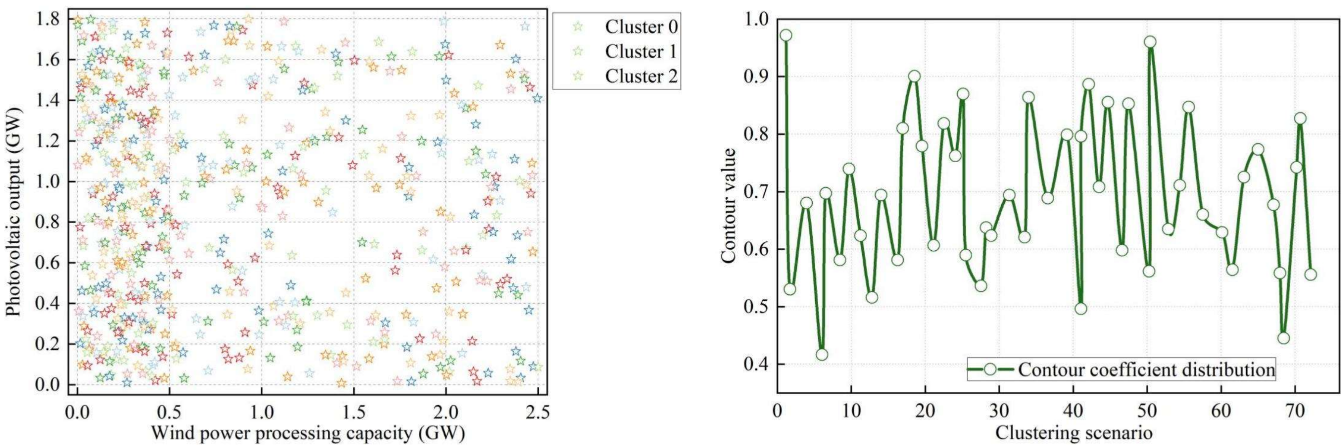

(a) Center of clustering (b) Clustering scenario

Figure 6: K-means scene clustering result graph

IV. B. 2) Screening of reactive power compensation points

The integrated L-Q sensitivity of each node under the differentiated scenarios is calculated in the distribution network, the nodes with higher integrated L-Q sensitivity under each scenario are counted, and the 10 simulation scenarios are combined and the five points with the highest frequency are selected. The CLQSI values are calculated for each node in all scenarios and shown in Fig. 7. Here, regarding the setting of k, it is considered that the configuration of reactive power sources at each node is complete and the upper and lower limits of the operation constraints are wide, and $k_j = 1/q$ is taken. The black color block indicates that the CLQSI value is negative, which means that the node accesses the reactive power in this scenario, which will make the static voltage stability of the system decrease, and meanwhile, for the nodes from 19-25, the CLQSI value is lower in each scenario, reflecting that the accessed reactive power affects the static stability of the node. access to reactive power has less impact on the static stability of the node, while nodes 14 and 31 have achieved larger values of CLQSI in nearly all scenarios, so they are included in the consideration.

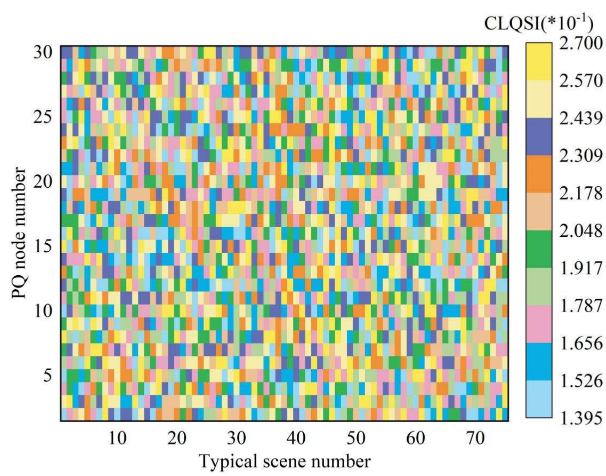

Figure 7: *CLQSI* of all nodes in the entire scene

IV. B. 3) Analysis of compensation effects

When the distributed wind power is not connected to the system, the network loss of the distribution network obtained by using the Newton Ruff current calculation is 245 kW, the voltage offset is 4.8882 p.u., and the voltage amplitude of each node in the system is shown in Fig. 8.

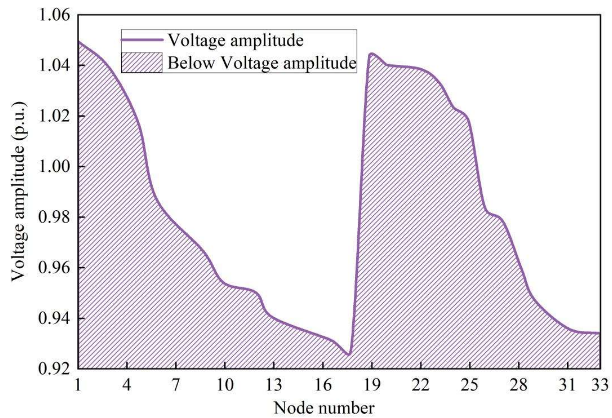

Figure 8: Point voltage amplitude when the fan is not connected

It can be seen from the figure that the voltage is at the regional minimum at node 17 and node 31 respectively, this is due to the fact that there are certain constraints on the capacity of the generators, transformers and other equipment in the system, but the load demand in the system is high, making the reactive power insufficient. According to the voltage standard, the deviation of supply voltage cannot deviate from 10%. Therefore, when part of the system voltage is below 0.95 p.u, the reactive power output needs to be enhanced and reactive power optimization measures need to be taken.

To further explore the influence of compensation on voltage quality under the multi-objective reactive power optimization model and solution method designed in this paper, calculations were conducted for 10 typical scenarios generated respectively. Table 1 shows the (I1) network loss cost (yuan), (I2) voltage offset (p.u.), (I3) network loss reduction (%), and (I4) voltage offset reduction (%) of the 10 scenarios calculated by the method proposed in this paper before and after compensation.

Table 1: Scene optimization result

Scene	Before compensation		After compensation		Compensation effect	
	I1	I2	I1	I2	I3	I4
A1	102.1828	4.7184	72.3937	3.695	29.15	21.69
A2	93.9438	4.6703	64.1547	3.6469	31.71	21.91
A3	81.5498	4.1055	51.7607	3.0821	36.53	24.93
A4	90.4808	4.5414	60.6917	3.518	32.92	22.53
A5	90.5548	4.4051	60.7657	3.3817	32.90	23.23
A6	99.5118	4.5421	69.7227	3.5187	29.94	22.53
A7	94.0078	4.2049	64.2187	3.1815	31.69	24.34
A8	87.2038	4.6412	57.4147	3.6178	34.16	22.05
A9	108.1808	4.6058	78.3917	3.5824	27.54	22.22
A10	92.7648	4.4509	62.9757	3.4275	32.11	22.99

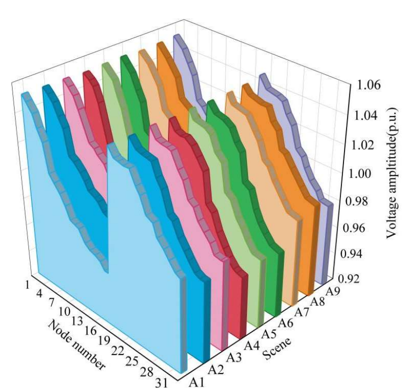

Figure 9: The average voltage of each scene after compensation

It can be seen that under the optimization of the method model and the square solution method in this paper, the network loss cost and voltage offset of the 10 scenarios have decreased to different degrees. The net loss reduction effect is most obvious in (A3) scene 3 (36.53%), and the voltage offset optimization effect is best in (A7) scene 7 (24.34%).

The average voltage of each scene after compensation is shown in Fig. 9, and it can be seen more clearly that the voltages of all scenes are at 0.92 p.u. and above, where the lowest voltage is located in (A4) scene 4 at 0.9657.

V. Conclusion

Based on the structure and characteristics of distribution network, this paper builds a multi-objective reactive power optimization model and proposes an improved sparrow search algorithm based on multi-strategy fusion as the solution method.

The proposed multi-objective reactive power optimization model and solution method in the simulation experiments, it is suggested that decentralized access or end-of-feeder access should be used when the PV penetration rate is small to improve the overall voltage level of the distribution network. When the PV penetration rate is too large, branch node access or feeder end access should be used to minimize the number of nodes that exceed the upper voltage limit of the distribution network. In the application of actual scenarios, it can assist different scenarios to improve the compensation effect, in which the network loss decreases up to 36.53%, the voltage offset optimization up to 24.34%, and at the same time ensures that all the scenarios have a voltage of 0.92p.u. and above.

References

[1] Kumar, S., & Rathore, K. (2023). Renewable energy for sustainable development goal of clean and affordable energy. International Journal of Materials Manufacturing and Sustainable Technologies, 2(1), 1-15.

[2] Østergaard, P. A., Duic, N., Noorollahi, Y., & Kalogirou, S. (2022). Renewable energy for sustainable development. Renewable energy, 199, 1145-1152.

[3] Iweh, C. D., Gyamfi, S., Tanyi, E., & Effah-Donyina, E. (2021). Distributed generation and renewable energy integration into the grid: Prerequisites, push factors, practical options, issues and merits. Energies, 14(17), 5375.

[4] Mehigan, L., Deane, J. P., Gallachóir, B. Ó., & Bertsch, V. (2018). A review of the role of distributed generation (DG) in future electricity systems. Energy, 163, 822-836.

[5] Wang, C., & Li, P. (2010). Development and challenges of distributed generation, the micro-grid and smart distribution system. Dianli Xitong Zidonghua/Automation of Electric Power Systems, 34(2), 10-14+.

[6] Li, C., Zhou, H., Li, J., & Dong, Z. (2020). Economic dispatching strategy of distributed energy storage for deferring substation expansion in the distribution network with distributed generation and electric vehicle. Journal of Cleaner Production, 253, 119862.

[7] Rozon, F., McGregor, C., & Owen, M. (2023). Long-term forecasting framework for renewable energy technologies' installed capacity and costs for 2050. Energies, 16(19), 6874.

[8] Zhu, Y., Zhang, J., Hu, Y., Cui, F., & Chu, W. (2021, November). Research on Optimization of Power System Regulation Capacity Based on New Energy Installed Capacity. In Journal of Physics: Conference Series (Vol. 2095, No. 1, p. 012018). IOP Publishing.

[9] Lakshmi, G. S., Rubanenko, O., Divya, G., & Lavanya, V. (2020, October). Distribution energy generation using renewable energy sources. In 2020 IEEE India Council International Subsections Conference (INDISCON) (pp. 108-113). IEEE.

[10] Manditereza, P. T., & Bansal, R. (2016). Renewable distributed generation: The hidden challenges–A review from the protection perspective. Renewable and Sustainable Energy Reviews, 58, 1457-1465.

[11] Adajah, Y. Y., Thomas, S., Haruna, M. S., & Anaza, S. O. (2021, July). Distributed Generation (DG): a review. In 2021 1st international conference on multidisciplinary engineering and applied science (ICMEAS) (pp. 1-5). IEEE.

[12] Eltamaly, A. M., Mohamed, Y. S., El-Sayed, A. H. M., & Elghaffar, A. N. A. (2019). Impact of distributed generation (DG) on the distribution system network. Annals of the Faculty of Engineering Hunedoara, 17(1), 165-170.

[13] Karabiber, A., Keles, C., Kaygusuz, A., & Alagoz, B. B. (2013). An approach for the integration of renewable distributed generation in hybrid DC/AC microgrids. Renewable energy, 52, 251-259.

[14] Adefarati, T., & Bansal, R. C. (2019). Energizing renewable energy systems and distribution generation. In Pathways to a smarter power system (pp. 29-65). Academic Press.

[15] Yazdani, A., & Dash, P. P. (2009). A control methodology and characterization of dynamics for a photovoltaic (PV) system interfaced with a distribution network. IEEE Transactions on Power Delivery, 24(3), 1538-1551.

[16] Quraan, M., Samara, Q., Favuzza, S., & Zizzo, G. (2017, June). Impact of integrating photovoltaic based DG on distribution network harmonics. In 2017 IEEE International Conference on Environment and Electrical Engineering and 2017 IEEE Industrial and Commercial Power Systems Europe (EEEIC/I&CPS Europe) (pp. 1-5). IEEE.

[17] Silva, E. N., Rodrigues, A. B., & da Silva, M. D. G. (2016). Stochastic assessment of the impact of photovoltaic distributed generation on the power quality indices of distribution networks. Electric Power Systems Research, 135, 59-67.

[18] Fu, X., Chen, H., Cai, R., & Yang, P. (2015). Optimal allocation and adaptive VAR control of PV-DG in distribution networks. Applied Energy, 137, 173-182.

[19] Saad, N. M., Sujod, M. Z., Lee, H. M., Abas, M. F., Jadin, M. S., Ishak, M. R., & Abdullah, N. R. H. (2018). Impacts of photovoltaic distributed generation location and size on distribution power system network. International Journal of Power Electronics and Drive Systems, 9(2), 905.

[20] Beckstedde, E., & Meeus, L. (2023). From "fit and forget" to "flex or regret" in distribution grids: dealing with congestion in European distribution grids. IEEE power and energy magazine, 21(4), 45-52.

[21] Series, I. E. T. R. E. (2009). Microgrids and active distribution networks. The institution of Engineering and Technology, 332.
[22] Xia, S., Bu, S., Wan, C., Lu, X., Chan, K. W., & Zhou, B. (2018). A fully distributed hierarchical control framework for coordinated operation of DERs in active distribution power networks. IEEE transactions on power systems, 34(6), 5184-5197.
[23] Abdeltawab, H. H., & Mohamed, Y. A. R. I. (2017). Mobile energy storage scheduling and operation in active distribution systems. IEEE Transactions on Industrial Electronics, 64(9), 6828-6840.
[24] Galvez, C., & Abur, A. (2020). Fault location in active distribution networks containing distributed energy resources (DERs). IEEE Transactions on Power Delivery, 36(5), 3128-3139.
[25] Fahad, S., Goudarzi, A., Bo, R., Waseem, M., Al-Ammari, R., & Iqbal, A. (2024). A Robust Demand Regulation Strategy for DERs in a Single-Controllable Active Distribution Network. IEEE Systems Journal.
[26] Oikonomou, K., Parvania, M., & Khatami, R. (2019). Deliverable energy flexibility scheduling for active distribution networks. IEEE Transactions on Smart Grid, 11(1), 655-664.
[27] Zheng, W., Wu, W., Zhang, B., Sun, H., & Liu, Y. (2015). A fully distributed reactive power optimization and control method for active distribution networks. IEEE Transactions on Smart Grid, 7(2), 1021-1033.
[28] Ding, T., Yang, Q., Yang, Y., Li, C., Bie, Z., & Blaabjerg, F. (2017). A data-driven stochastic reactive power optimization considering uncertainties in active distribution networks and decomposition method. IEEE Transactions on Smart Grid, 9(5), 4994-5004.
[29] Go, S. I., Yun, S. Y., Ahn, S. J., & Choi, J. H. (2020). Voltage and reactive power optimization using a simplified linear equations at distribution networks with DG. Energies, 13(13), 3334.
[30] Xu, P., Song, D., Song, Y., Cheng, L., & Xie, J. (2024, July). Sequential linear programming-based parameter optimization of dynamic reactive power compensation devices for security enhancement and new energy power transmission increasing. In 20th International Conference on AC and DC Power Transmission 2024 (ACDC 2024) (Vol. 2024, pp. 883-888). IET.
[31] Zhang, C., Chen, H., Liang, Z., Guo, M., Hua, D., & Ngan, H. (2017). Reactive power optimization under interval uncertainty by the linear approximation method and its modified method. IEEE Transactions on Smart Grid, 9(5), 4587-4600.
[32] Qu, L., Zhang, S., Lin, H. C., Chen, N., & Li, L. (2020). Multiobjective Reactive Power Optimization of Renewable Energy Power Plants Based on Time-and-Space Grouping Method. Energies, 13(14), 3556.
[33] Lopez, J. C., Contreras, J., Munoz, J. I., & Mantovani, J. R. S. (2012). A multi-stage stochastic non-linear model for reactive power planning under contingencies. IEEE Transactions on Power Systems, 28(2), 1503-1514.
[34] Amrane, Y., Boudour, M., & Belazzoug, M. (2015). A new hybrid technique for power systems multi-facts optimization design. International transactions on electrical energy systems, 25(11), 2961-2981.
[35] Soler, E. M., Asada, E. N., & Da Costa, G. R. (2013). Penalty-based nonlinear solver for optimal reactive power dispatch with discrete controls. IEEE transactions on power systems, 28(3), 2174-2182.
[36] Saxena, N. K., & Kumar, A. (2017). Dynamic reactive power compensation and cost analysis for isolated hybrid power system. Electric Power Components and Systems, 45(18), 2034-2049.
[37] Rather, Z. H., Chen, Z., Thøgersen, P., & Lund, P. (2014). Dynamic reactive power compensation of large-scale wind integrated power system. IEEE Transactions on Power Systems, 30(5), 2516-2526.
[38] Paramasivam, M., Salloum, A., Ajjarapu, V., Vittal, V., Bhatt, N. B., & Liu, S. (2013). Dynamic optimization based reactive power planning to mitigate slow voltage recovery and short term voltage instability. IEEE Transactions on Power Systems, 28(4), 3865-3873.
[39] Shen, X., Liu, Y., & Liu, Y. (2018). A multistage solution approach for dynamic reactive power optimization based on interval uncertainty. Mathematical Problems in Engineering, 2018(1), 3854812.
[40] Jaisiva, S., Prabaakaran, K., Kumar, C., Lakshmanan, M., Alwabli, A., Jaffar, A., ... & Miyajan, A. (2023). A novel solution for the optimal reactive power dispatch problem using an artificial neural network integrated with the firefly optimization algorithm. Frontiers in Energy Research, 11, 1310010.
[41] Alonso, F. R., Oliveira, D. Q., & De Souza, A. Z. (2014). Artificial immune systems optimization approach for multiobjective distribution system reconfiguration. IEEE Transactions on Power Systems, 30(2), 840-847.
[42] Sarvaiya, J., & Chudasama, M. (2017). Multi-objective planning for optimal allocation of DG and RPC units in radial distribution system using genetic algorithm. In ICRISET 2017?: International Conference on Research and Innovations in Science, Engineering Kalpa Publications in Engineering (Vol. 1, pp. 485-476).
[43] Linlin, Y., Lihua, Z., Gaojun, M., Feng, Z., & Wanxun, L. (2022). Research on multi-objective reactive power optimization of power grid with high proportion of new energy. IEEE Access, 10, 116443-116452.
[44] Dong, P., Xu, L., Lin, Y., & Liu, M. (2017). Multi-objective coordinated control of reactive compensation devices among multiple substations. IEEE Transactions on Power Systems, 33(3), 2395-2403.
[45] Ganguly, S. (2014). Multi-objective planning for reactive power compensation of radial distribution networks with unified power quality conditioner allocation using particle swarm optimization. IEEE Transactions on Power Systems, 29(4), 1801-1810.